Quantitative X-Ray Microanalysis of Thin NiO Films by Monte Carlo and Cliff-Lorimer Methods

Aldo Armigliato,[1]* Stefano Frabboni,[2] Gian Carlo Gazzadi,[3] and Rodolfo Rosa[4]
[1]CNR-IMM Institute, Via P.Gobetti, 101 40129 Bologna (Italy)
[2]Dipartimento di Fisica, Università di Modena e Reggio Emilia, Via G. Campi 213/A, 41100 Modena (Italy) and CNR-Istituto di Nanoscienze-S3, via G. Campi 213/A, 41100 Modena, Italy
[3]CNR-Istituto di Nanoscienze-S3, via G. Campi 213/A, 41100 Modena, Italy
[4]Dipartimento di Scienze Statistiche, Università di Bologna, Via Belle Arti, 40126 Bologna (Italy)

*armigliato@bo.imm.cnr.it

https://doi.org/10.1017/S1551929514000054 Published online by Cambridge University Press

Introduction

Thin-film X-ray microanalysis in the scanning transmission electron microscope (STEM) is often performed by depositing the material of interest onto an amorphous carbon film supported by a transmission electron microscope (TEM) grid. Quantification of the concentration of the various elements in such a bi-layer (or perhaps stack of films) is possible by Monte Carlo methods only and not by the available analytical methods, unless the contributions of all but one layer are negligible. The analytical methods, which can treat only samples consisting of a single film, include the popular Cliff-Lorimer (C-L) approach [1], which yields the composition of a *single* film from properly determined *k*-factors. This method requires an independent measurement of the film thickness when the X-ray absorption correction is significant, as in the case of the OK X-ray line in the NiO film investigated in this paper. Different methods have been proposed in the literature to determine both film thickness and composition of a *single* layer [2, 3]. In any case, to apply the C-L method, *experimental k*-factors (no absorption) must be determined; this can be accomplished by fabricating a wedge-shaped standard film (NiO in our case) and applying the so-called extrapolation method [4, 5].

In this article we first demonstrate that, in the case of a stack of NiO and C layers, the best accuracy is obtained by a Monte Carlo (MC)-based quantification procedure [6, 7]. Secondly, we show a way that quantification is also possible by the C-L approach, which is less accurate because over/under layers cannot be taken into account. In the C-L case, experimental *k*-factors must be obtained; we accomplish this here by applying the extrapolation method [5] to a wedge-thinned NiO/Ni lamella, fabricated by the FIB technique.

Monte Carlo-Based Quantification

The application of the MC method to X-ray microanalysis is based on the comparison between experimental data and corresponding values obtained by computer simulations. It is important to note that, in the case of a binary film AB of thickness *t*, there are two unknowns (concentration and thickness) and only one experimental value, intensity ratio I(A)/I(B).

Briefly, let $I^j(A)$ and $I^j(B)$ be the measured X-ray intensities, where $j = 1, 2$ refers to two different experimental conditions. As an example, in the 2 tilt-angle method [6, 8, 11], data are obtained by performing the analysis at two different orientations of the sample, and the intensity ratios $R^j_{exp} = I^j(A) / I^j(B)$ are computed. The next steps are the following: (a) the generation by an MC code of two sets of corresponding computed ratios of X-ray intensities $R^j_{calc}(C, t)$ as a function of the film concentration and thickness and (b) the minimization of the difference $|R^j_{calc}(C, t) - R^j_{exp}|$ to obtain the point estimates of *C* and *t*.

The physical model of the MC code (see [7] and references therein) adopts the single-scattering approach in which the angular deflection is determined by the elastic scattering and the energy loss between scattering points is given by the continuous slowing down approximation of the Bethe law. The Wentzel potential is employed to derive the cross section for elastic collisions. The relativistic Bethe stopping power has been adopted to describe energy dissipation by electrons in the target. The code can deal with any film thickness in multilayer systems. When the path between two subsequent collisions crosses one, it is rescaled using the mean-free-path ratio in each layer. The X-ray intensity is calculated at each electron scattering event by means of the ionization cross section Q, the fluorescence yield ω, the weight of the line p, the absorption in the sample, and in the detector (ε).

Materials and Methods

NiO/C test sample. The NiO/C test specimen proposed by Egerton and Cheng [9] for the characterization of analytical electron microscopes has been employed in our experiments. It is commercially available from Emitech Ltd (**NiOX™**, www.emitech.co.uk) and consists of a thin film of NiO_x (x~1) deposited onto amorphous carbon and supported by a 200-mesh molybdenum grid. The relevant thickness values for our specific sample (batch D) are 55 nm for the NiO_x film (density 6.7 g/cm^3) and 20 nm for the carbon layer. Prior to its insertion into the microscope, the specimen was plasma-cleaned for 2 min in a Fischione instrument (Model 1020) to remove surface hydrocarbon contamination.

Preparation of the NiO/Ni wedge lamella standard. We started from a commercial bulk, <100> oriented, Ni cylindrical sample (Goodfellow Cambridge Ltd., England, www.goodfellow.com), 12 mm in diameter, and 2 mm thick. Its purity was guaranteed to be better than 99%. A 350 µm thick slice was removed from the cylinder by spark erosion, followed by an electropolishing step to remove the resulting damaged back zone (about 40 µm). After having removed the surface oxide from this slice by a mechanical treatment, followed by an annealing in an atmosphere of slight Ar overpressure, it was subjected to a thermal treatment at 650°C for 4 hours in a furnace for surface oxidation, in order to obtain a NiO film thickness in the 1 micrometer range. Rutherford backscattering spectrometry (RBS) analysis, performed with a 2 MeV beam of He^+ ions, yielded a thickness of 0.75 µm for the NiO film overlying the Ni bulk, with an

MAIA3

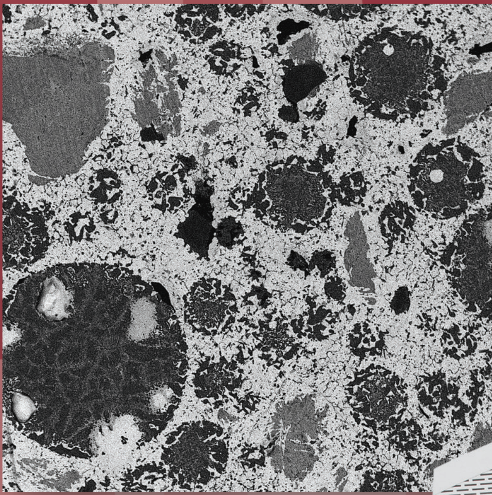

Do you seek higher resolution imaging?
Discover the imaging capabilities of the TESCAN MAIA today.

www.tescan-usa.com

TESCAN USA, 508 Thomson Park Drive, Cranberry Twp., PA 16066, Tel: 724-772-7433, Email: info@tescan-usa.com

https://doi.org/10.1017/S1551929514000054 Published online by Cambridge University Press

https://doi.org/10.1017/S1551929514000054 Published online by Cambridge University Press

oxygen concentration of C(O) = 50 ± 2 at%, that is, nearly stoichiometric, as expected. This sample was then inserted into the FIB equipment (FEI Dual Beam Strata 235M, www.fei.com).

The lamella was prepared using the FIB lift-out method [10]. The details are reported in a previous paper [11]. At the end of this process the lamella was attached to a special TEM grid by Pt FIB deposition and released from the tip by FIB cut. Thinning and wedge shaping of the lamella were performed at this stage. A low-current FIB ion beam was repeatedly scanned parallel to the sidewalls, along a line advancing toward the center of the lamella. This procedure resulted in sidewall cleaning of material deposited during the milling and Pt-deposition steps and in a thinning of the lamella. The wedge shape was obtained by rotating the scan line by 6° with respect to the lamella axis. A lateral and a top view of the wedge-shaped lamella are shown in Figure 1 and Figure 2, respectively. The NiO/Ni interface is clearly evidenced by the dashed line in Figure 2. It does not look like a straight line in this SEM image, yet it consists of two segments, the left one being inclined in the wedged region; this is due to a projection effect of the wedge, as observed with a tilt angle of 57°.

As previously reported [11], by properly choosing the milling conditions, no stoichiometry change detectable by EDS was introduced into TEM lamellas by the FIB preparation; no peak from the Ga^+ ion beam was detected in the X-ray spectra.

Experimental STEM+EDS details. A 200 kV FEI Tecnai F20 FEG-(S)TEM, equipped with a high-angle annular dark-field (HAADF) detector, the TIA (Tecnai Interface Analysis) software, and an EDAX Sapphire Si(Li) detector, were employed for X-ray microanalysis of both the NiO/C sample and the NiO region of the wedge-FIBed NiO/Ni lamella. The acquisition of X-ray spectra was performed in several areas of the NiO/C sample and along 10-point linescans (3 µm long) in the case of the lamella, using in both cases an electron beam current of 1 nA in a 1 nm spot, in a stationary mode; no damage induced by this high-current density was observed. The CK, OK, and SiK integrated peak intensities were obtained by the ES Vision software (Emispec Systems Inc, www.fei.com) of the microscope.

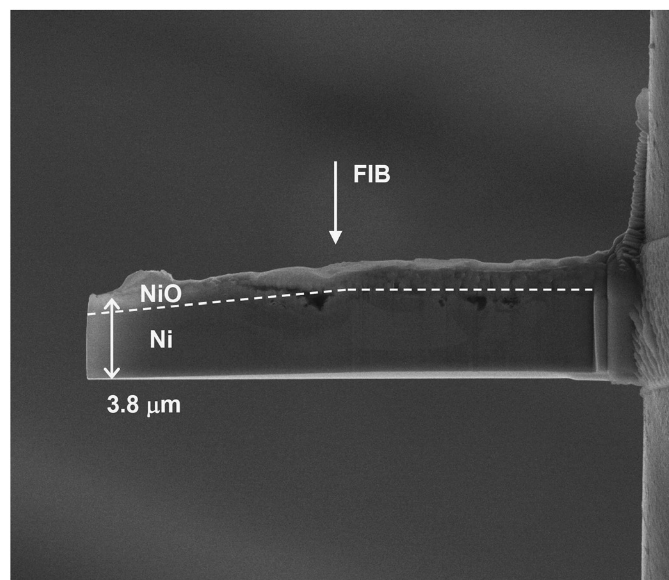

Figure 1: Lateral view of the NiO/Ni lamella. The NiO thickness (left) varies from 120 nm to 160 nm. The NiO/Ni interface is evidenced (see text for details). The direction of the STEM beam is perpendicular to the image plane, the FIB direction is shown. Reprinted with permission from Cambridge University Press, © 2013, see [11].

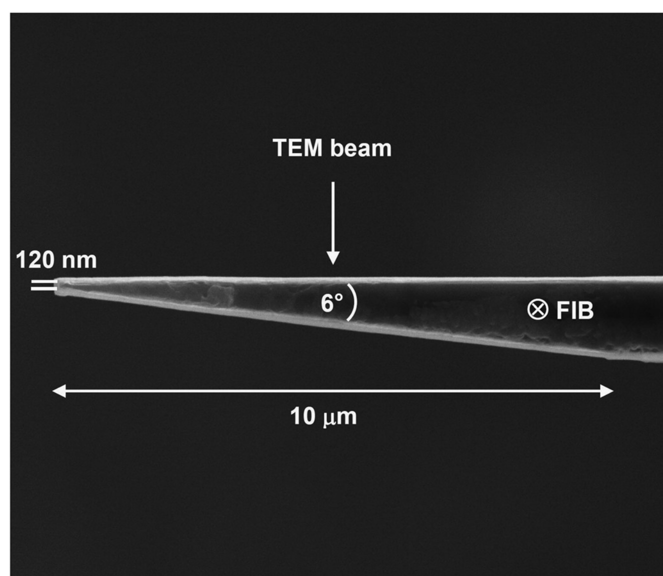

Figure 2: Top view of the lamella, showing the 10 µm long wedge. The local thickness at the apex of the wedge is ranging from 120 nm (top) to 320 nm (bottom). The FIB (and TEM e-beam) directions are shown. Reprinted with permission from Cambridge University Press, © 2013, see [11].

For the MC analysis, three different specimen tilt angles toward the detector were used: 10°, 15°, and 20°, whereas the C-L analysis, based on the extrapolation technique, was performed only at a 20° specimen tilt. Because of the need for analyzing both the NiO film and the 20 nm thick amorphous carbon layer, and to minimize carbon contamination, the sample temperature was kept at 100°K during the analysis by using a Gatan LN_2-cooled double-tilt holder. The anti-contamination cold finger was also used in both cases to further prevent sample contamination. To reduce sample drift during the analysis, the automatic anti-drift correction, available in the TIA software by FEI, was employed.

Results

Analysis of the NiO/C test sample by MC method. Figure 3 shows a sketch of the investigated sample in the two possible orientations with respect to the incident electron beam of the STEM: grid downward (Figure 3a) and grid upward (Figure 3b). Accordingly, the C layer is below (a) or above (b) the NiO film. Although only the former is recommended for general analysis, mounting the sample in both orientations successively was useful for our MC analysis of the bilayer. In addition, as it will be shown later on, the result of this test can be extended to the detection of a carbon contamination overlayer and to its effect on the NiO film quantification.

From spectra obtained in the two configurations [7], the difference in the CK and OK peak intensity between the two geometries is clearly visible. From the net peak intensities, three ratios, I(NiK)/I(OK), I(NiK)/I(CK), and I(OK)/I(CK), were obtained. These were the experimental data inputs to our MC code.

https://doi.org/10.1017/S1551929514000054 Published online by Cambridge University Press

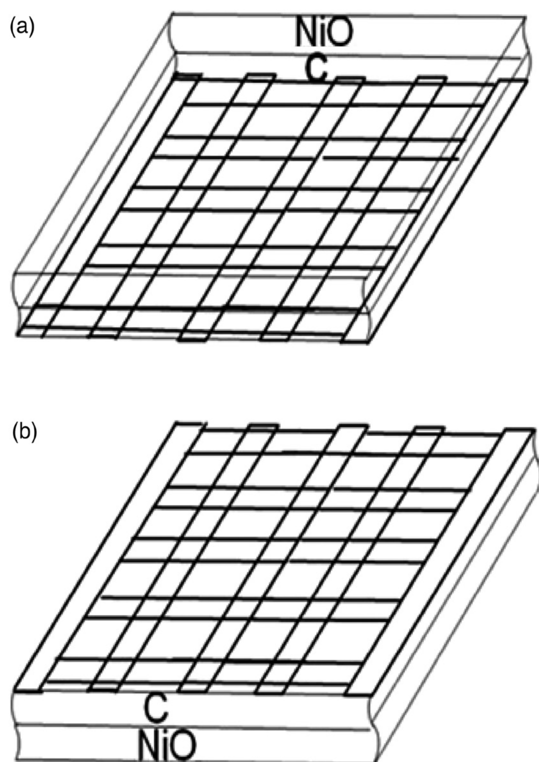

Figure 3: Sketch of the investigated NiO film, deposited on a C-coated Mo grid to show the different loading in the microscope holder. (a) grid (and C layer) below the NiO film (grid downward); (b) grid above the NiO film (grid upward). Though this latter geometry is not recommended in normal quantitative analysis, it has been analyzed by our MC method to determine the effect of a C-overlayer on the oxygen concentration in the NiO film (see text for details). Reprinted with permission from Cambridge University Press, © 2009, see [7].

To estimate the O concentrations and the local film thickness, we employed the above-mentioned 2 tilt-angle method, previously described in [6, 8]. We have chosen two couples of tilt angles, namely 10°–20° and 15°–20°. The former increases the differential X-ray absorption, whereas, the latter reduces the possible shadowing effect due to the specimen holder. From these results for the two geometries (Table 1), it was deduced that the oxygen concentration is in agreement with the one certified by Emitech (C(O) = 50 ± 2 at%), in the grid-downward geometry, whereas a significant deviation is obtained in the grid-upward case. This could be due to the presence of a carbon contamination on the sample surface.

An alternative hypothesis is that the values of the physical parameters (in particular, ionization cross sections Q and detector efficiency ε) are inaccurate. But this would also affect the concentrations obtained by the 2 tilt-angle method in the grid downward geometry, which is not the case. We have also checked the absence of ice contamination in front of the detector window.

To check the hypothesis of the carbon contamination, we simulated by the 2 tilt-angle method a geometry in which, besides considering both grid positions, there is a further carbon film on the sample surface, with thickness t^*_C ranging from 10 nm to 30 nm. Table 2 shows that a 20–30 nm thick carbon overlayer yields similar results for both geometries, in agreement with the certified values. To further confirm this, we have used MC to obtain calculated (I(OK)/I(NiK), I(OK)/I(CK), and I(NiK)/I(CK)) intensity ratios, assuming a stoichiometric NiO composition and t^*_C varying from 0 nm to 30 nm. With t^*_C at about 20 nm, the agreement between the MC-calculated intensity ratios and the experimental intensity ratios is satisfactory in both geometries (Table 3). We point out that in Table 3 "experimental" refers to the ratios among the net integrated intensities, as obtained from the application of the ES Vision software to the experimental spectra. Obviously, a quantification can also be performed by this software (C-L method) starting from the intensities, but it is neither used in this work, nor needed for the MC calculations.

Table 1: Estimates and associated errors of O concentration C_O (at.%) and thickness t (nm) of the NiO film obtained by the MC 2 tilt-angle method, with the angle couples: 10°–20° and 15°–20°.

	Grid Position			
	Downward		Upward	
Tilt Angles	C_O (at.%)	t (nm)	C_O (at.%)	t (nm)
10°–20°	50.5 ± 1.5	60 ± 20	53.5 ± 1.0	52 ± 10
15°–20°	50.3 ± 1.3	43 ± 18	52.4 ± 1.0	62 ± 14

Analysis of the NiO/Ni standard by C-L approach. Figure 4 shows a STEM image taken in the NiO region of the lamella obtained by the FIB thinning of the surface-oxidized bulk Ni standard, together with the X-ray spectra taken in 10 points along the 3 μm linescan shown as a straight line. The crosses at the end points of the linescan correspond to the position where the first and tenth spectra have been taken, which are reported in (b) and (c), respectively. The red square box was used for the antidrift correction by the cross-correlation method. The OK and the NiK peaks were used for quantification purposes. It is worth noting that no GaK peak from the Ga ion beam of the FIB is visible.

According to [5], the procedure to get *k*(O-Ni) is based on the following steps:

a) The 10 spectra are quantified with the C-L equation, assuming a stoichiometric composition and putting all *k*-factors equal to 1, under the thin-film approximation (no absorption).
b) A plot of C(O) and C(Ni) concentrations versus net NiK X-ray intensity is drawn.
c) The chart is fitted with a linear trendline.
d) The trendline, *extrapolated* to zero thickness, represents a *virtual* concentration.
e) Dividing the *true* concentration ratio by the *virtual* concentration ratio yields the measured *k*(O-Ni) factor. Namely, $k(\text{O-Ni})^{wt}$ or $k(\text{O-Ni})^{at}$ values will be obtained for *true* concentrations given in wt% or at%, respectively.

In our case, linear extrapolation of OK and NiK intensities to zero yields C(O) = 21.6 ± 0.7 and C(Ni) = 78.4 ± 0.7 (*virtual* concentrations, Figure 5), respectively, as:

$$k(\text{O-Ni}) = \frac{[C(\text{O})/C(\text{Ni})]stoichiometric}{[C(\text{O})/C(\text{Ni})]virtual}$$

This results in $k(\text{O-Ni})^{wt}$ = 0.99 and $k(\text{O-Ni})^{at}$ = 3.63. These *experimental* values are quite different from the $k(\text{O-Ni})^{wt}$ = 1.30 *theoretical* value calculated by the ES Vision software

https://doi.org/10.1017/S1551929514000054 Published online by Cambridge University Press

Table 2: Estimates and associated errors of O concentration C_O (at.%) and thickness t (nm) of the NiO film, obtained by the MC 2 tilt-angle method, with a t^*_C thick carbon contaminating film on the sample surface.

		Grid Position			
		Downward		**Upward**	
	Tilt Angles	**C_O (at.%)**	**t (nm)**	**C_O (at.%)**	**t (nm)**
t^*_C = 10 nm	10°–20°	49.8 ± 1.3	51 ± 17	52.9 ± 1.7	38 ± 16
	15°–20°	50.1 ± 1.3	49 ± 18	52.2 ± 1.0	46 ± 10
t^*_C = 20 nm	10°–20°	49.0 ± 1.2	50 ± 18	49.8 ± 1.2	59 ± 16
	15°–20°	49.1 ± 1.1	44 ± 15	50.2 ± 1.0	54 ± 10
t^*_C = 30 nm	10°–20°	48.3 ± 1.4	52 ± 18	49.3 ± 1.2	45 ± 11
	15°–20°	48.2 ± 1.3	45 ± 19	49.0 ± 1.7	56 ± 19

Table 3: Experimental and MC-generated intensity ratios I(OK)/I(NiK), I(OK)/I(CK), and I(NiK)/I(CK). Tilt angle α = 20°.

	Grid Position					
	Downward			**Upward**		
Intensity Ratios	$\frac{I(OK)}{I(NiK)}$	$\frac{I(OK)}{I(CK)}$	$\frac{I(NiK)}{I(CK)}$	$\frac{I(OK)}{I(NiK)}$	$\frac{I(OK)}{I(CK)}$	$\frac{I(NiK)}{I(CK)}$
Experimental	0.309 ± 0.005	2.46 ± 0.06	8.0 ± 0.3	0.251 ± 0.005	0.99 ± 0.02	3.95 ± 0.05
t^*_C (nm)	**MC-Generated Intensity Ratios**					
0	0.30	10.33	34.47	0.27	3.08	11.40
10	0.29	3.91	13.74	0.26	1.96	7.64
20	0.27	2.33	8.62	0.24	1.41	5.78
30	0.26	1.62	6.93	0.23	1.08	4.65

(corresponding to $k(\text{O-Ni})^{at}$ = 4.77). It must be also noted that the contribution to the primary OK intensity from the secondary fluorescence by the NiL X rays is of the order of 10^{-3}, thus quite negligible [11]. Finally, we observe that to obtain k(O-Ni) values, this method does not require the knowledge of the detector efficiency ε (unlike MC [see previous paragraph], and the C-L method based on *theoretical k* factors).

Analysis of the NiO/C test sample by the C-L method. Let us now turn back to the NiO/C test sample. Having determined the experimental k value, the quantification of the NiO test sample by the C-L method can be repeated with better accuracy. The analysis was carried out by determining the OK and NiK X-ray intensities from spectra taken in this film, in both the grid-downward and grid-upward geometry, in the same experimental conditions as in the above-reported experiment on the wedge FIB lamella. The calculation of the Ni-O film composition, performed in the former geometry assuming the above-reported absorptionless $k(\text{O-Ni})^{at}=3.63$ value and an absorption correction calculated by MC for a thickness of 55 nm, yields an oxygen concentration in agreement with the 2 tilt-angle MC method (Table 4). This result confirms the correctness of the *experimental* C-L factor k value obtained in this paper.

A quite different NiO composition is found by the C-L method in the grid-upward geometry. In this case the deviation from the stoichiometry is about 11 at%. This clearly indicates the inherent limitation of this analytical method, which assumes that the sample consists of a single, ternary C-O-Ni film. A still worse quantification can be expected for overlayers consisting of elements heavier than carbon.

In Table 4 the O and Ni concentrations (at.%) are summarized. They were obtained by the two methods (MC and C-L) in the two geometries.

Discussion

The most accurate and reliable quantification of thin films by X-ray microanalysis in a (S)TEM can be obtained if the contribution to the experimental spectra of any carbon layer placed above and/or below a binary alloy is taken into account. This is particularly important when the sample contains light elements. To this end, application of the MC method [6, 8] has proven to be useful because, unlike analytical approaches such as the C-L method, it can treat a specimen consisting of a stack of thin films. In fact, MC can accurately calculate the X rays *generated* in each layer according to the ionization cross section of the different elements at every step of the electron trajectories. The number of *transmitted* X rays is obtained applying the proper absorption correction. In contrast with MC, given a spectrum containing three or more peaks (CK, OK, NiK, and NiL in our case), the C-L method infers that the sample consists of a single, ternary C-O-Ni film. This leads to an inaccurate quantification of the film of interest when it is covered by one or more overlayers.

In this work we used a standard NiO sample deposited onto a grid covered with a carbon support film. From the OK and NiK intensities measured in the experimental spectra taken in the two possible sample geometries (grid downward and grid upward), MC calculation yields a NiO film composition in good agreement with the certified one only

https://doi.org/10.1017/S1551929514000054 Published online by Cambridge University Press

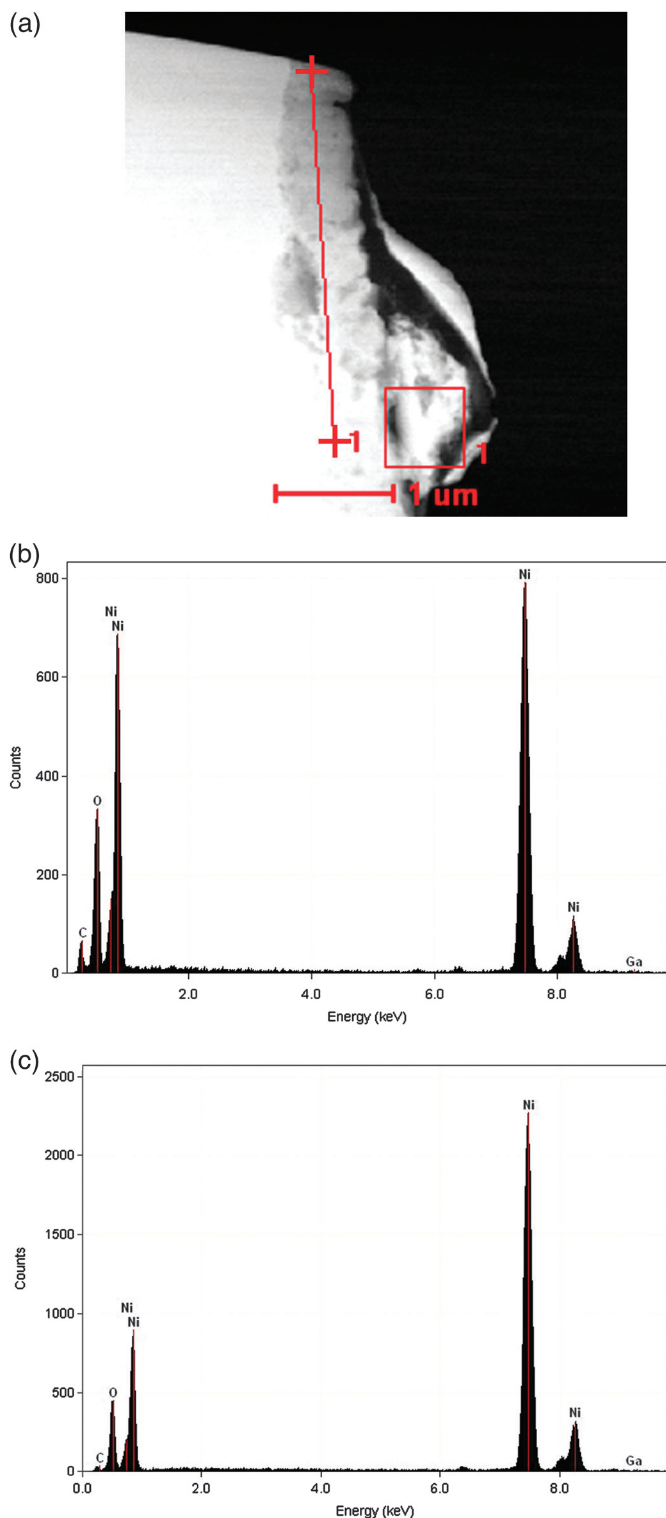

Figure 4: STEM image of the NiO/Ni lamella and EDS spectra taken on a 3000 nm long linescan. (a): the NiO film is almost vertical and clearly distinguishable from the bulk Ni substrate on its left. The two red crosses correspond to the thinnest (top) and the thickest (marked as 1) analyzed points, respectively. The square box on the right (also marked #1) is used by the software TIA of the Tecnai STEM for the drift correction with the cross-correlation method. (b) EDS spectrum taken in the thinnest point of the linescan. In addition to the OK and the NiK (and NiL) peaks, a small carbon peak is visible. (c) EDS spectrum taken in the thickest point of the linescan. Note the much higher vertical full-scale value with respect to the spectrum on the left. Tilt angle: α=20°. Reprinted with permission from Cambridge University Press, © 2013, see [11].

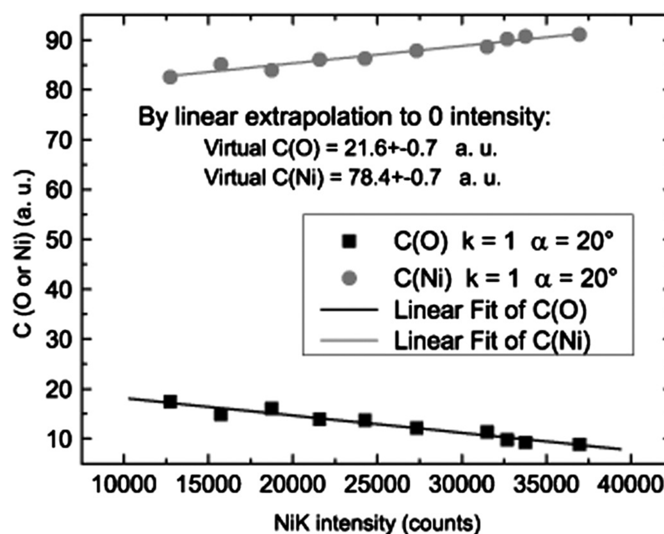

Figure 5: Plot of O and Ni concentrations versus NiK intensity, generated in the different points in the linescan. The curves are fitted with a linear trendline. The extrapolation to zero intensity (thickness) yields *virtual* concentrations, where from the experimental C-L coefficient *k*(O-Ni) can be calculated (see text for details) [10].

Table 4: Comparison between the MC and C-L concentrations obtained from the NiO test sample in the two geometries.

Concentration	Grid Downward		Grid Upward	
(at.%)	MC[a]	C-L[b]	MC[a]	C-L[b]
C(O)	49	49	50	44
C(Ni)	51	51	50	56

[a]2-tilt method, assuming t^*_C is about 20 nm; [b]with *experimental* k(O-Ni)^{at} = 3.63.

in the former case. However, if also the C-K experimental intensity is included in the MC simulations, it turns out that the a full agreement is obtained by assuming the presence of a contamination C overlayer at the sample surface (in both geometries).

As mentioned above, the C-L method could not be applied to this situation as it can treat only samples consisting of *one* layer. However, if the sample is mounted in the grid-downward geometry, MC shows that the influence on the NiO composition of the carbon overlayer is not significant.

It is important to *experimentally* determine the *k*(O-Ni) factors when using the C-L method. The best way, in our opinion, is to fabricate a wedge-thinned NiO/Ni standard by FIB milling. This allows one not only to obtain the factor by the extrapolation method, but also to check its correctness by calculating the Ni and O concentration in the different analyzed points; the absorption correction can be easily evaluated because the local thickness can be accurately measured on the basis of the wedge geometry.

Conclusions

The quantitative X-ray microanalysis by (S)TEM of a commercial, certified, 55 nm thick NiO film, deposited on a 20 nm carbon layer, has been performed by both the MC and the C-L methods. The presence of a few tens nm thick carbon contamination at the sample surface, revealed by MC,

does not affect significantly the NiO quantification when working in proper experimental conditions. This makes the C-L method applicable, even though, unlike MC, it cannot analyze stacks of films. The required *k*(O-Ni) C-L factors have been experimentally determined by the extrapolation method applied to a wedge-shaped lamella, thinned by the FIB technique.

References

[1] G Cliff and G Lorimer, *J Microsc* 103 (1975) 203–07.
[2] Z Horita et al., *Phil Mag* A59 (1989) 939–52.
[3] M Watanabe and DB Williams, *J Microsc* 221 (2006) 89–109.
[4] Z Horita et al., *J Microsc* 143 (1986) 215–31.
[5] E Van Cappellen, *Microsc Microstruct Microanal* 1 (1990) 1–22.
[6] A Armigliato and R Rosa, *Ultramicroscopy* 32 (1990) 127–36.
[7] R Rosa and A Armigliato, *X-ray Spectrom* 18 (1989) 19–23.
[8] A Armigliato and R Rosa, *Microsc Microanal* 15 (2009) 99–105.
[9] RF Egerton and SC Cheng, *Ultramicroscopy* 55 (1994) 43–54.
[10] LA Giannuzzi et al., *Mat Res Soc Symp Proc* 480 (1997) 19.
[11] A Armigliato et al., *Microsc Microanal* 19 (2013) 79–84.

MT

THE NEW DESK V
THE GOLD STANDARD IN SAMPLE PREPARATION

Now upgraded with storage for up to ten recipes and a color touch screen display, the Desk V HP delivers breakthrough electron microscopy sample preparation.

DENTONVACUUM
BARRIERS BECOME BREAKTHROUGHS

Visit us at:
www.dentonvacuum.com/mt

https://doi.org/10.1017/S1551929514000054 Published online by Cambridge University Press

JSM-7100F/LV • JSM-7100FT/LV • JSM-7500F • JSM-7610F • JSM-7800F/LV

FE SEM
7000 SERIES

CHOOSE THE PERFECT FE SEM FOR ALL YOU DO

- *outstanding low kV/low vacuum performance*
- *high resolution imaging and nanoanalysis of structures, surface details, and magnetic samples*
- *high stable current with double condenser lens and aperture angle control lens*
- *multi-port chamber for in situ nanolab utility*

Budget-conscious labs and leading-edge research centers will find the ultra versatility, performance, and support to be the perfect fit.

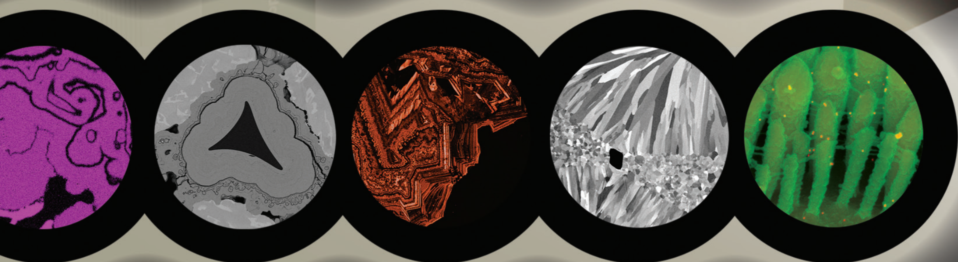

EDS Backscatter CL Backscatter Mixed SEBSE*

* Courtesy of Dr. Artur Indzhykulian, Harvard Medical School

JEOL
www.jeolusa.com
salesinfo@jeol.com
978-535-5900

Solutions for Innovation

www.jeolusa.com/FESEM

https://doi.org/10.1017/S1551929514000054 Published online by Cambridge University Press